# Frustrating Quantum Batteries

A.G. Catalano,[1,2] S.M. Giampaolo,[1] O. Morsch,[3] V. Giovannetti,[4,5] and F. Franchini[1,*]

[1] *Institut Ruđer Bošković, Bijenička cesta 54, Zagreb 10000, Croatia*

[2] *Université de Strasbourg, 4 Rue Blaise Pascal, Strasbourg 67081, France*

[3] *Consiglio Nazionale delle Ricerche (CNR)–Istituto Nazionale di Ottica (INO) and Dipartimento di Fisica dell'Università di Pisa, Largo Pontecorvo 3, Pisa 56127, Italy*

[4] *NEST, Scuola Normale Superiore and Istituto Nanoscienze—CNR, Pisa I-56126, Italy*

[5] *Planckian, Pisa I-56125, Italy*

(Received 11 July 2023; revised 28 May 2024; accepted 2 July 2024; published 30 July 2024)

We propose to use a quantum spin chain as a device to store and release energy coherently and we investigate the interplay between its internal correlations and outside decoherence. We employ the quantum Ising chain in a transverse field and our charging protocol consists of a sudden global quantum quench in the external field to take the system out of equilibrium. Interactions with the environment and decoherence phenomena can dissipate part of the work that the chain can supply after being charged, measured by the ergotropy. We find that overall, the system shows remarkably better performance, in terms of resilience, charging time, and energy storage, when topological frustration is introduced by setting antiferromagnetic interactions with an odd number of sites and periodic boundary conditions. Moreover, we show that in a simple discharging protocol to an external spin, only the frustrated chain can transfer work and not just heat.

DOI: 10.1103/PRXQuantum.5.030319

## I. INTRODUCTION

In recent years, there has been a global surge of interest in harnessing quantum phenomena at the microscopic level, driven by the rapid advancement of new quantum technologies [1,2]. One of the fundamental questions that have been addressed is that of energy storage and transfer at the quantum level, keeping in mind possible adverse effects that can interfere. Within the context of energy storage, an intriguing area of exploration that has attracted considerable attention recently is the study of "quantum batteries" [3–11], which are quantum mechanical systems designed for energy storage. Quantum batteries (QBs) utilize quantum effects to achieve more efficient and rapid charging processes compared to classical systems, by circumventing the need to physically move the energy carriers through driven diffusion. This burgeoning field of research encompasses numerous intriguing questions, ranging from the stabilization of stored energy [12,13] to the investigation of optimal charging protocols [14–21]. One of the first practical implementations of this type of device is the quantum Dicke battery in Ref. [6], where the energy from a photonic cavity mode (acting as a charger) is transferred to a battery comprising $N$ quantum units, each described by a two-level system. Such a model exhibits a collective speed-up [22] in the charging process. The Dicke battery has garnered significant interest due to its versatility in various implementation platforms (e.g., superconducting qubits [23], quantum dots [24,25], coupled with a microwave resonator, Rydberg atoms in a cavity [26], etc.), leading to the exploration of numerous variations of this model [27–36].

To have a practical application, QBs must, however, not only rapidly store energy but also be able to provide useful energy (i.e., work) once charged [9,37–39]. A crucial aspect of the problem is to assess the stability of these models in realistic scenarios where they are subject to environmental noise. Preliminary studies in this direction have been obtained in Refs. [12,40–54] where various schemes have been proposed to stabilize QBs in the presence of specific types of perturbations. In Refs. [14–17], a general theory of work extraction for noisy QB models composed of large collections of noninteracting subsystems (quantum cells) have been presented. The fundamental theoretical tool for this type of study is provided by the *ergotropy* [55,56], a nonlinear functional that gauges the maximum amount of energy that can be extracted from an assigned

*Contact author: fabio@irb.hr, gfabio@gmail.com

input state of a quantum system under reversible—i.e., unitary—operations that do not alter the system entropy.

Inspired by this whole activity, with this work we would like to contribute to the field of quantum energy storage and transfer. However, while in the literature part of the interest around QBs has been directed toward providing energy to macroscopic systems, more recently some efforts have also been directed toward situations in which quantum fluctuations play a dominant role with respect to thermal fluctuations [19,43,57–60]. Following this line, we specialize on devices operating purely in a quantum setting. We present a many-body system that can be charged through a change in the external magnetic field and used to transfer energy onto a second target system. Most of all, we consider the effect of certain dephasing to show the resilience of the energy stored in the battery against time. In our investigation, we are driven by the observation that in the future it might be hard to design a universal quantum machine able to withstand any type of decoherence and dephasing and it will be necessary to combine several devices able to perform different tasks, while being optimized for resilience against different external conditions. Thus, we propose a protocol to start the development of such a cluster of devices, starting with the most basic quantum thermodynamic task. We introduce a sort of an activator for a series of quantum devices with which it exchanges energy. Since this device will share most of the properties of a QB, in the following we will also refer to it as a quantum battery. However, we would like to stress that while QBs based on the Dicke model have already shown some important results in terms of scalability [36], we will defer the investigation of these properties for our device to a subsequent work, since now we are focused on describing the merit of its energy exchange with other quantum devices, not with macroscopic systems.

In particular, we analyze the work extraction from a system made of $N$ interacting spins which, once charged, undergo complete dephasing in the energy eigenbasis of the associated Hamiltonian. More precisely, our analysis is focused on many-body models that exhibit exotic behavior when proper frustrated boundary conditions (FBCs) are imposed. A typical example is represented by a linear chain of an odd number of spins arranged in a ring geometry (i.e., with periodic boundary conditions): when classically paired with antiferromagnetic (AFM) interactions, such a system cannot realize the perfect Néel ordering [61–63] and hence exhibits topological frustration due to the presence of a ferromagnetic (FM) kink along the chain. At the quantum level, the introduction of such frustration radically modifies the structure of both the ground-state manifold [64–66] and the low-energy spectrum [67], leading to a whole set of novel forms of behavior [68–71], which are potentially interesting for technological applications. One important example is that while in nonfrustrated models (at least, far from critical points) the ground-state manifold is separated by a finite energy gap from the rest of the spectrum, for the topologically frustrated systems it belongs to a band (in fact, for the ring geometry discussed above the gap closes as $N^{-2}$).

As a charging mechanism, we consider a simple (and relatively easy to implement) global quantum quench. Moreover, we show how topological frustration enhances the robustness to decoherence of a quantum battery: while in the nonfrustrated case, the ergotropy of the battery can be reduced to less than 30% of its initial value by decoherence phenomena, we observe that a frustrated battery manages to retain more than 90% of the original ergotropy in all the parameter ranges analyzed. Finally, we propose a simple discharging protocol that shows how it is possible to transfer energy from a many-body quantum battery charged with our protocol to an ancillary spin. Surprisingly, we observe that only frustrated batteries can transfer work efficiently, in the form of ergotropy, while the nonfrustrated battery only manages to heat up the ancillary system.

The paper is organized as follows. in Sec. II, we introduce the quantum spin models and the charging protocol that we consider to realize a quantum battery, as well as introducing the role of decoherence in these systems. In Sec. III, we compare the performance of frustrated and nonfrustrated batteries under the assumption of *fast charging*, i.e., considering a purely coherent charging protocol. In Sec. IV, we drop this assumption and analyze the effect of decoherence during the charging protocol, introducing nonunitary dynamics during the quantum quench. In Sec. V, we present a protocol for energy transfer from a many-body quantum battery to a single ancillary spin. Finally, we discuss our results and possible developments in Sec. VI.

## II. THEORETICAL FRAMEWORK

### A. The model

While the phenomenology of topological frustration has already been described in detail for more general models such as the *XYZ* chain [66], without loss of generality, here we will focus on the simplest case, i.e., a ring of an odd number $N$ of spin-1/2 particles coupled via the quantum Ising chain in a transverse magnetic field. The Hamiltonian of such a model is

$$H(J,h) = J\sum_{l=1}^{N}\sigma_l^x\sigma_{l+1}^x - h\sum_{l=1}^{N}\sigma_l^z, \tag{1}$$

where the $\sigma_l^\alpha$ ($\alpha = x, y, z$) are Pauli operators acting on the $l$th spin, $\sigma_{N+1}^\alpha = \sigma_1^\alpha$ enforces the periodic boundary conditions, and $h$ is the strength of the external field. The constant $J$ governs the nature of the couplings among the spins: its modulus $|J|$ determines the strength of the Ising interactions, while its sign allows us to tune from an AFM

frustrated system, for $J > 0$, to a nonfrustrated FM one for $J < 0$. In the rest of our analysis, we will fix $|J| = 1$, so that all the energies and times are measured in units of $|J|$ and $1/|J|$, respectively.

Regardless of the sign of $J$, the model is analytically integrable and a detailed solution can be found in Appendix A. Due to this, it is possible to observe how while some properties of the system are not affected by the presence or absence of topological frustration, others assume very different forms of behavior. An example of the latter is the existence of an energy gap between the ground-state manifold and the closest set of excited states in the ordered phase $|h| < 1$. If, in the nonfrustrated case, in the thermodynamic limit the twofold ground-state manifold is separated from the band of excited states by a finite energy gap equal to $\Delta_{\mathrm{FM}} = 1 - |h|$, this disappears completely in the presence of frustration. In fact, for $J = 1$, at finite sizes, the ground state is part of a band made of $2N$ states in which the gap between the two lowest-energy elements closes according to the law

$$\Delta_{\mathrm{AFM}} = \frac{|h|}{2(1-|h|)}\frac{\pi^2}{N^2} + O(N^{-4}). \tag{2}$$

Hence, the frustrated AFM model presents a gap that vanishes quadratically with the system size in the frustrated phase. While this expression is correct for $|h| < 1$, as we approach the critical points $h_c = \pm 1$, new corrections grow on the right-hand side of Eq. (2) and eventually the gaps of the frustrated and nonfrustrated models tend to coincide and both close as $N^{-1}$ near to criticality.

### B. The charging protocol

To store energy in a spin system as the one described in Eq. (1), i.e., to use such a system as a QB, we propose a simple protocol based on quenches of the external magnetic field sketched in Fig. 1. The starting point is the ground state $|\epsilon_0\rangle$ with associated energy $\epsilon_0$ of the Hamiltonian $H_0 = H(J, h_0)$. Such a Hamiltonian admits a set of eigenstates that we denote as $\{|\epsilon_\ell\rangle\}$, ordered in such a way that the associated eigenvalues $\epsilon_l$ satisfy the condition $\epsilon_\ell \leq \epsilon_{\ell+1}$. At time $t = 0$, we perform a sudden global quench to the Hamiltonian $H_1 = H(J, h_1)$, the eigenstates of which we denote by $\{|\mu_k\rangle\}$, ordered in such a way that $\mu_k \leq \mu_{k+1}$. The system then evolves unitarily under the action of $H_1$ for a certain time interval $\tau$, after which the system Hamiltonian is quenched back to $H_0$ to close the charging cycle. Note that $h_1$ can also be greater than $|J| = 1$ crossing the Ising quantum critical point and thus the charging process can also happen in a different phase, before we return to $h_0$. In the absence of external interference, the QB at the end of the charging process is described by the vector $|\psi(\tau)\rangle = e^{-\imath H_1 \tau}|\epsilon_0\rangle$ and the energy stored is

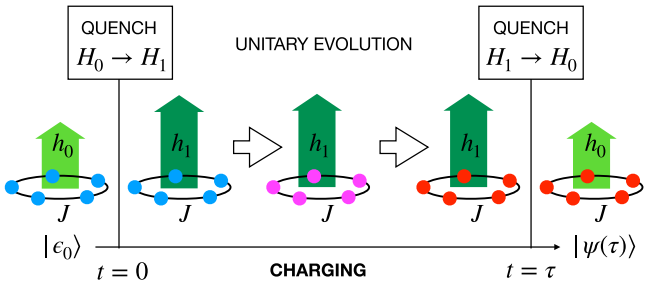


FIG. 1. A schematic overview of the charging process: the QB is represented by a collection of an odd number $N$ of spin-1/2 particles, initialized in the ground state $|\epsilon_0\rangle$ of the Ising Hamiltonian $H_0 = H(J, h_0)$ with local field $h = h_0$ and coupling $J$, the modulus of which is equal to 1. Setting $J = -1$ corresponds to considering a nonfrustrated ferromagnetic (FM) QB model, while setting $J = 1$ corresponds to a frustrated AFM QB. Energy is pumped into the system by quenching the local field from $h_0$ to $h_1$ at time $t = 0$. The system then evolves during the time interval $[0, \tau]$ via the unitary evolution associated with the Hamiltonian $H_1 = H(J, h_1)$. Finally, the external field is restored to its original value $h_0$ at $t = \tau$.

given by

$$E_{\mathrm{in}} = \langle\psi(\tau)|H_0|\psi(\tau)\rangle - \epsilon_0 = \sum_\ell P_\ell(\tau)(\epsilon_\ell - \epsilon_0), \tag{3}$$

where the populations $P_\ell(\tau)$ are

$$P_\ell(\tau) = \left|\sum_k e^{-i\mu_k\tau}\,\langle\mu_k|\,|\epsilon_0\rangle\,\langle\epsilon_\ell|\,|\mu_k\rangle\right|^2. \tag{4}$$

Due to the integrability of the Hamiltonian in Eq. (1), it is possible to derive analytically the populations $P_\ell(\tau)$ (for details, see Appendix B). In Fig. 2, we plot $P_\ell(\tau)$ for both the frustrated and nonfrustrated cases, for a specific choice of the system parameters. From the figure, it is possible to observe that at the level of the populations of the eigenstates of $H_0$, there is no clear difference between the two cases. As a further consequence, the amount of energy stored in the system is almost the same, with small differences that can be made to vanish by increasing the system size.

### C. The role of decoherence

As long as the evolution of the system remains unitary, it is always possible to reverse it, hence completely recovering the stored energy $E_{\mathrm{in}}$. But in the presence of decoherence, the dynamics of a quantum system become nonunitary and hence there is no unitary transformation that can bring the system back to its initial state, thereby reducing the amount of energy that can be extracted from it [55,56]. However, one of the main problems in the study of decoherence is that the results obtained are, in

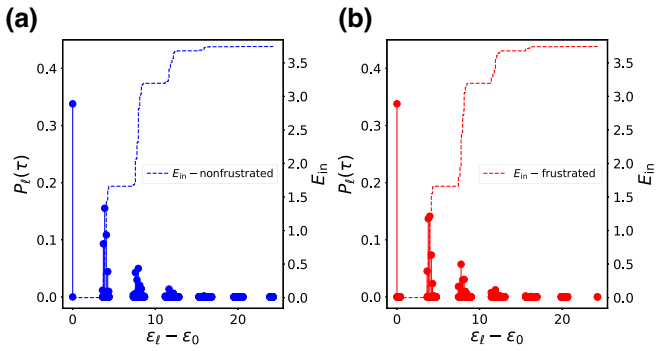


FIG. 2. A plot of the distribution $P_\ell(\tau)$ of Eq. (4), which defines the populations of the energy eigenspaces of the QB Hamiltonian $H_0 = H(J, h_0)$ after a cyclic quench from $h_0 = 0.1$ to $h_1 = 0.8$ and back to $h_0$, for the (a) nonfrustrated ($J = -1$) and (b) frustrated ($J = 1$) systems. The dashed lines represent the partial energy contributions to $E_{\rm in}$, defined in Eq. (3), due to the occupied states up to that spectral energy. These results are obtained for a chain of $N = 13$ spins, setting $\tau = 0.5$.

general, strongly dependent on the nonunitary-dynamics model taken into account which, in turn, depends on the specifics of the experimental apparatus in which the model is tested. To carry out our theoretical analysis, we have chosen to consider, as a source of decoherence, purely dephasing dynamics such as that induced by the master equation proposed by Milburn [72]:

$$\dot{\rho}(t) = -i[H(t), \rho(t)] - \frac{1}{2\nu}[H(t), [H(t), \rho(t)]]. \qquad (5)$$

Here, $\rho(t)$ and $H(t)$ are the instantaneous system density matrix and Hamiltonian, $\dot{\rho}(t)$ is the derivative of the density matrix, and $\nu$ parametrizes the characteristic decoherence rate of the model. Note that in principle, the latter could depend on the parameters of the Hamiltonian and the system size.

Taking into account the charging process that we have introduced, and hence the dependence on time of the Hamiltonian, the second term on the right-hand side of Eq. (5) implies that the off-diagonal terms of the density matrix in the energy eigenbasis, characterized by finite oscillation frequencies, are exponentially suppressed with a characteristic decoherence time equal to $\tau_{k,l} \approx (2\nu/(\Delta E_{k,l}^2))$, where $\Delta E_{k,l}$ is the energy difference between the states $|\epsilon_k\rangle$ $|\epsilon_l\rangle$ (or $|\mu_k\rangle$ $|\mu_l\rangle$ when we consider a slow-charging process). While each entry decays at its own rate, it is possible to characterize some general collective behavior. In order to do so, let us remark that the global quench $H_0 \leftrightarrow H_1$ preserves all the symmetries of the Hamiltonian, most importantly the translational and the parity symmetry along $z$, with the parity operator, defined as $\Pi^z = \prod_{l=1}^N \sigma_l^z$. Therefore, since the initial state $|\epsilon_0\rangle$ is an eigenstate of the momentum operator with zero momentum and fixed parity, the occupied states $\epsilon_\ell$ with $P_\ell(\tau) \neq 0$ are also eigenstates with the same parity as the ground state and vanishing momentum [70] and they are never degenerate, implying that all the relevant $\Delta E_{k,l}$ values always differ from zero. As a consequence, after a sufficiently long time, due to the effect of the nonunitary dynamics, the state of the QB will be well approximated by a diagonal density matrix with zero coherence in the eigenbasis of the Hamiltonian [for a formal solution of Eq. (5), see Appendix C]. From Fig. 2, we can see that states with a nonvanishing population are distributed across different energy bands and thus their energy difference can be classified as either intraband or interband. The energy differences $\Delta E_{k,l}$ between states belonging to different bands scale as $2(J - h)$ (with only subleading corrections dependent on $N$): if an off-diagonal term $\rho_{k,l}$ is related to two states coming from different bands, the time scale of its exponential suppression, which we call the *fast decoherence time* $\tau_1$, has a functional dependence of the type $\nu/(J - h)^2$ on the parameters of the system, with subleading finite-size $N$-dependent corrections. On the contrary, if the two states $|\epsilon_k\rangle$ and $|\epsilon_l\rangle$ belong to the same energy band, their energy difference is smaller, dependent on their relative position within the band, and also changing with the chain length $N$. Accordingly, their decoherence time scale will be much larger, resulting into an overall *slow decoherence time* $\tau_2 \gg \tau_1$. The existence of two different time scales in the nonunitary dynamics induced by Eq. (5) can be appreciated by looking at Fig. 3, in which we depict the behavior of the relative entropy of coherence for the state $\rho(t)$, i.e., the $C_{\rm RE}(\rho(t))$ [73], and provide an estimate of $\tau_{1,2}$ for some choice of parameters. The relative entropy of coherence is defined as

$$C_{RE}(\rho(t)) = S(\rho_D(t)) - S(\rho(t)), \qquad (6)$$

where $S(x) = -\sum_i \lambda_i \log \lambda_i$ is the von Neumann entropy of the density matrix $x$, with eigenvalues $\{\lambda_i\}$, and $\rho_D(t)$ is the diagonal matrix obtained by $\rho(t)$ artificially suppressing all the off-diagonal elements in a given basis (the Hamiltonian eigenbasis in our case). From the plot, it is easy to see the existence of two very different time scales. A heuristic fit on our numerical data shows that, indeed, $\tau_1$ shows a subleading dependence on $N$, while the linear growth of $\tau_2$ with the system size can be interpreted as arising from the average intraband energy difference, which should go as $1/N$, since each band hosts of the order of $N$ states in a finite width. Note that these estimates and fits are highly heuristic and valid only for system sizes of the order of those for which we have data, since a straightforward extrapolation to the thermodynamic limit would yield absurd projections. Nonetheless, since we are interested in finite systems, they suffice for our purposes.

The estimation of these times allows us to identify different operating regimes for the QB. Since, ideally, a QB should be able to store energy for a long time, we have

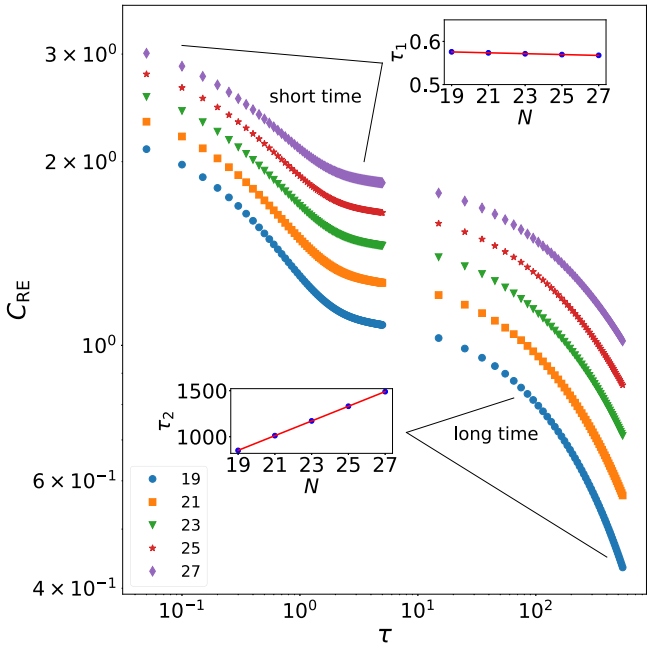


FIG. 3. A plot of the entropy of coherence in Eq. (6) as a function of time under the decoherence dynamics of Eq. (5). We observe the emergence of two distinct decoherence time scales: a fast one, characterized by a short time $\tau_1$, which is weakly dependent on $N$, and a slower one with characteristic time $\tau_2 \gg \tau_1$, which instead is proportional to $N$. Data have been obtained for $J = 1$, $h_0 = 0.1$, $\Delta h = 0.5$, and $\nu = 10$. The results are the same for the frustrated and nonfrustrated systems. Quantitatively, from a best-fit analysis we find that $\tau_1 \approx 0.048(\nu/((J - h_0)^2)) + 0.001N$, while $\tau_2 \approx 80.8N - 688$.

determined that, in this paper, we will focus on the worst-case scenario, i.e., one in which an attempt is made to extract work after a time $T \gg \tau_2$ has passed since the end of the charging process, and we leave a detailed analysis of the time scales $\tau_{1,2}$ and of the forms of behavior for intermediate times for future work. In this long-time scenario, the decoherence leads to the complete collapse of the QB density matrix into a diagonal ensemble in the energy eigenbasis of the system. On the other hand, with regard to the charging process, we will specifically examine two distinct charging regimes. The first of these is the so-called *fast-charging regime*, in which the charging time $\tau$ is considered to be much faster than that of any decoherence time $\tau \ll \tau_1$. As a consequence, the charging process can be considered a unitary process. On the other hand, in the *slow-charging regime*, in which $\tau_1$ and $\tau$ are comparable, partial dephasing also occurs during the charging process.

## III. FAST-CHARGING REGIME

In the fast-charging regime (i.e., for $\tau_1 \gg \tau$), we can neglect the effect of the dephasing during the charging process. Under this hypothesis, the asymptotic state of the QB that emerges from Eq. (5) at time $T \gg \tau_2$ corresponds to the completely incoherent (in the basis of the eigenstates of $H_0$) diagonal density matrix state

$$\rho(T) = \sum_\ell P_\ell(\tau)|\epsilon_\ell\rangle\langle\epsilon_\ell|, \tag{7}$$

where the $P_\ell(\tau)$ are the populations defined in Eq. (4).

Following the prescription of Refs. [55,56], the lowest-energy state that can be reached with (reversible) unitary processes acting on the density matrix $\rho(T)$ is its passive counterpart

$$\tilde{\rho}(T) = \sum_\ell \tilde{P}_\ell(\tau)|\epsilon_\ell\rangle\langle\epsilon_\ell|, \tag{8}$$

where the $\tilde{P}_\ell(\tau)$ are the eigenvalues of $\rho(T)$ rearranged in decreasing order ($\tilde{P}_\ell(\tau) \geq \tilde{P}_{\ell+1}(\tau)$). The energy that we can recover from the system via unitary operations can then be computed in terms of the system ergotropy, i.e., the difference between the energy of $\rho(T)$ and the mean energy of $\tilde{\rho}(T)$,

$$\begin{aligned} W &= \mathrm{Tr}(\rho(T)H_0) - \mathrm{Tr}(\tilde{\rho}(T)H_0) \\ &= \sum_\ell (P_\ell(\tau) - \tilde{P}_\ell(\tau))(\epsilon_\ell - \epsilon_0) \\ &= E_{\mathrm{in}} - \sum_\ell \tilde{P}_\ell(\tau)(\epsilon_\ell - \epsilon_0) = E_{\mathrm{in}} - E_{\mathrm{loss}}. \end{aligned} \tag{9}$$

The quantity $E_{\mathrm{loss}} = \sum_\ell \tilde{P}_\ell(\tau)(\epsilon_\ell - \epsilon_0)$ represents the amount of energy that we can no longer be extracted from the battery. Since $E_{\mathrm{loss}}$ is a positive quantity, we have that, due to the nonunitary dynamics acting after the end of the charge phase, the work $W$ that we can extract from the battery is less than the energy $E_{\mathrm{in}}$ stored in it. To quantify how robust the QB is toward decoherence, we compute the ratio between the amount of work that we can extract from it at time $T \gg \tau_2$ and the energy initially stored in the QB, i.e.,

$$\eta = \frac{W}{E_{\mathrm{in}}}. \tag{10}$$

The results obtained with a semianalytical approach (see Appendix B) are shown in Fig. 4. The results are obtained by maximizing $\eta$ throughout the charging time $\tau$ in the interval $[0, 50]$ in units of $1/|J|$. In Fig. 4(a), we depict the behavior of $\eta$ for a fixed value of $\Delta h = h_1 - h_0$ as a function of $h_0$, while in Fig. 4(b), we plot the result obtained keeping $h_0$ fixed and changing $\Delta h$.

As can be seen, in Fig. 4(a), well below the critical point $h_0 = 1$, the frustrated AFM battery is very resilient to the decoherence processes and, for a wide range of $h_0$, $\eta$ is close to 1 and well above 0.9. On the contrary, in the same

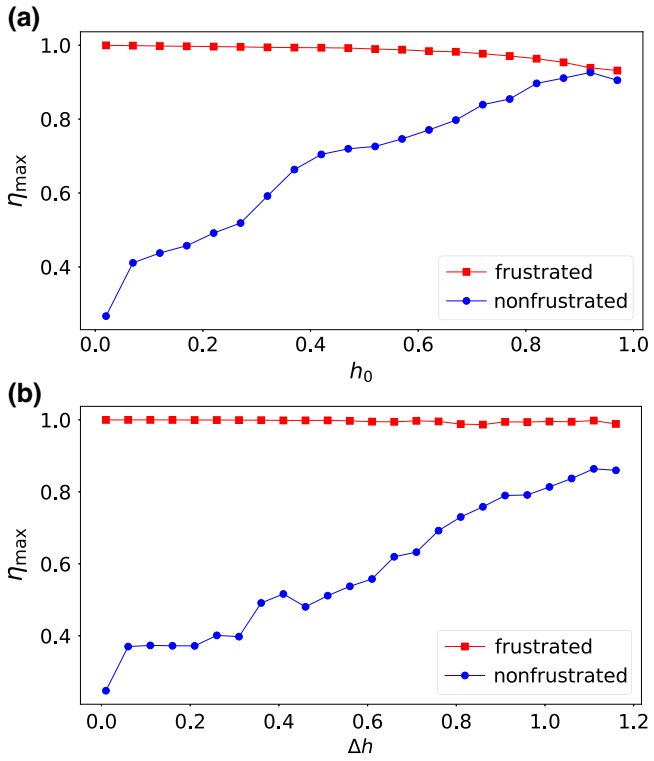


FIG. 4. The maximum value of $\eta$ defined in Eq. (10), computed (a) as a function of $h_0$ for $\Delta h = 0.01$ and (b) as a function of $\Delta h$ (lower panel) for $h_0 = 0.001$. Data are obtained for charging times $\tau \in (0, 50)$, for a chain of $N = 25$ spins. These plots show how, after decoherence, the frustrated chain has retained most of its charge, while the nonfrustrated one typically loses the majority of the initial charge.

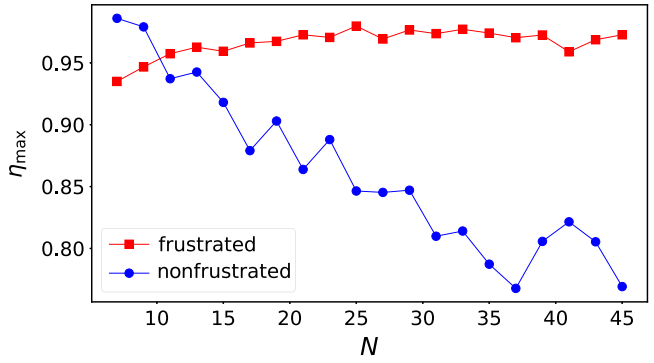


FIG. 5. The maximum value of $\eta$ in Eq. (10), computed for $\tau \in (0, 50)$, for the frustrated (red squares) and nonfrustrated (blue dots) Ising chain. Data are obtained for chains of size $N \in [7, 45]$, for $h_0 = 0.751$ and fixed $h_1 = 0.7$.

range of parameters, the loss in the work-extraction capability for an FM nonfrustrated QB can increase to 80%. Moreover, in Fig. 4(b), the value of $\eta$ for the frustrated battery is strikingly close to 1 in the whole range, while being considerably smaller for its nonfrustrated counterpart.

To understand the difference between the frustrated and nonfrustrated systems, we have to consider the different characteristics of their energy spectrum. In the magnetically ordered phase of nonfrustrated systems such as the one we are considering, the energy spectrum is characterized by two quasidegenerate states separated from the first band of excited states by a finite energy gap. Conversely, in frustrated systems, the ground state belongs to a band made of $2N$ states, the width of which is related to the value of the external field. By comparing these behaviors, taking into account the definition of $E_{\text{loss}}$, it is easy to explain the difference in behavior. Indeed, in the case of nontopologically frustrated models, the third term of the summation in the definition of $E_{\text{loss}}$ already provides a non-negligible contribution to the loss of extractable energy and, likewise, all the others that follow. Conversely, in frustrated systems, since all states belong to the same band, the contribution of the first $2N$ terms to $E_{\text{loss}}$ is small and it decreases as $|h_0|$ decreases. This greatly reduces the loss of energy that can be extracted from the battery and, consequently, increases $\eta$. However, when $|h_0|$ increases, the bandwidth of the frustrated model increases, reducing the value of $W$ and hence of $\eta$ while the gap of the ferromagnetic model narrows, resulting in an increment of $\eta$. These two different dependencies on $|h_0|$ explain why, close to the quantum critical point, the performance of the two systems becomes comparable. Moreover, since the number of states in the first band of the frustrated systems is proportional to the system size itself, it is natural to expect that the effect of reduction of the relative weight of $E_{\text{loss}}$ increases with $N$. This expected behavior is confirmed by the results shown in Fig. 5. In varying the system size, the value of $\eta$ of the frustrated system remains approximately constant, while it decreases with the system size for the nonfrustrated model.

A further parameter that is useful in characterizing the performance of the QB is the time needed to complete the charging process. For our protocol, there is a certain degree in arbitrariness in this choice. We have chosen to define the *charging time* as the one for which the first local maximum of the $E_{\text{in}}$ as a function of time is reached. This choice has been motivated by the empirical observation, supported by the plots presented in the Supplemental Material [74], that this time does not seem to scale with the system size and that subsequent maxima do not necessarily bring a significant improvement in energy. Moreover, this choice seems quite natural considering the necessity, inherent in the current status of quantum technologies, of keeping the charging time as short as possible. In Fig. 6, we show the results of an analysis of the charging time obtained varying $\Delta h$ for a fixed value of $h_0$. From the figure, we observe that regardless of the presence or absence of topological frustration in the system, the charging time generally decreases

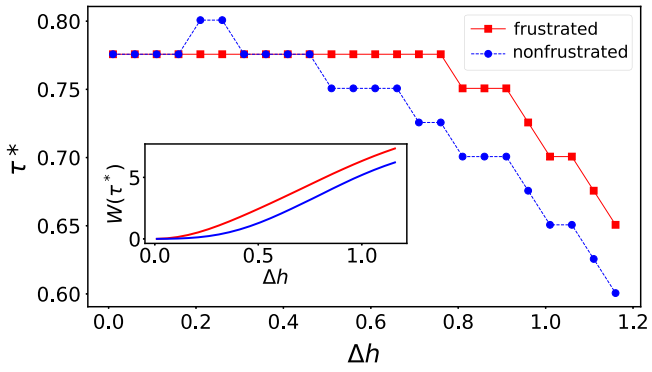


FIG. 6. The position of the first local time maximum $\tau^*$ and the corresponding value of $W$ (inset) for the frustrated (red) and nonfrustrated (blue) Ising chain. Data are obtained for a chain of $N = 25$ spins, for $h_0 = 0.001$ and $h_1 - h_0 \in (0.01, 1.2)$.

with increasing $\Delta h$, while the energy stored in the system increases. This fact gives rise to a virtuous circle in which the time required for this storage decreases as the energy stored by the system increases. Moreover, for frustrated systems, the ratio $\eta$ always remains greater than 0.8 and significantly higher than that of the nonfrustrated counterparts. This means that by increasing the jump in the external magnetic field, it is possible to charge the battery more, faster, and with higher resistance to decoherence. While this behavior is valid for both frustrated and nonfrustrated QBs, the data witness the fact that the performance of the former is always better than that of the latter.

## IV. SLOW-CHARGING REGIME

The results presented so far have been obtained under the hypothesis that the charging protocol is so fast that we can completely neglect any decoherence effects during charging. However, such a hypothesis is quite strong and an analysis of what happens when the charging process is affected by decoherence is mandatory. Therefore, in this section, we study the performance of our QB model in the slow-charging regime, in which the fast decoherence time $\tau_1$ and the charging time $\tau$ are comparable. To this end, we numerically integrate Eq. (5) during the charging time up to $\tau$. Even if, in this regime, the analysis is more complex, the basic concepts are the same as in Sec. III and we recover that, after the end of the charging process, waiting for a time $T \gg \tau_2$, the state of the QB reduces to a completely incoherent state of the form

$$\rho(T) \simeq \sum_{\ell} P'_{\ell}(\tau)|\epsilon_{\ell}\rangle\langle\epsilon_{\ell}|, \tag{11}$$

where the populations $P'_{\ell}(\tau)$ are

$$P'_{\ell}(\tau) = \sum_{k,k'} \langle\epsilon_{\ell}|\mu_k\rangle\langle\mu_k|\epsilon_0\rangle\langle\epsilon_0|\mu_{k'}\rangle\langle\mu_{k'}|\epsilon_{\ell}\rangle \times \exp[-\tfrac{(\mu_k-\mu_{k'})^2}{2\nu}\tau - i(\mu_k - \mu_{k'})\tau], \tag{12}$$

(for details, see Appendix C), which correctly reduces to Eq. (4) when all the exponential decays can be neglected. Note that although the derivation of Eq. (5) in Ref. [72] is not valid in the $\nu \to 0$ limit, we can take this limit of fast dephasing by instantaneously removing all off-diagonal contributions. However, one must be aware that taking the limit in this way implies the assumption that the quench that brings $h_0 \to h_1$ is instantaneous, i.e., $\Delta t_{quench} \ll \nu$. If this was not the case, then we might incur in a quantum Zeno effect [75], which would prevent the battery from charging. Since our protocol is based on instantaneous quantum quenches, we leave the investigation of the interplay between a finite quench speed and the decoherence speed to future work.

Similarly to what was done in Sec. III, we have compared the performance of the frustrated and nonfrustrated QB models using the ratio $\eta$ and the velocity of charging. We show the outcomes of the analysis in Fig. 7. For several values of the decoherence frequency $\nu$, we have charged the battery as a function of $\Delta h$, maximizing the robustness parameter $\eta = W/E_{\rm in}$ over time. As expected, by decreasing the decoherence frequency $\nu$, hence making the decoherence stronger and faster in destroying the coherence of the QB state, $\eta$ decreases but does not disappear completely—even in the limiting case $\nu = 0$, where all the off-diagonal elements of the density matrix are instantaneously suppressed soon after the quench of the external field from $h_0 \to h_1$. However, once again, the frustrated

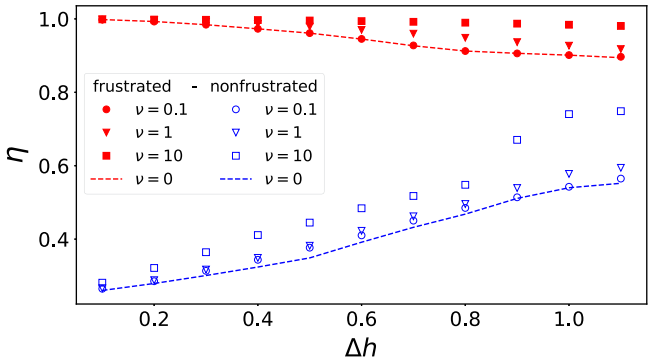


FIG. 7. The maximum in time of the robustness parameter $\eta$ for the frustrated (red) and nonfrustrated (blue) for a decoherent charging protocol, for different values of the decoherence frequency: $\nu = 10, 1, 0.1, 0$ (squares, triangles, circles, and dashed line). $\nu = 0$ corresponds to full decoherence, i.e., instantaneous convergence to the diagonal ensemble. Data are obtained for a chain of $N = 15$ spins, for $h_0 = 0.001$ and $h_1 - h_0 \in (0.02, 1.1)$.

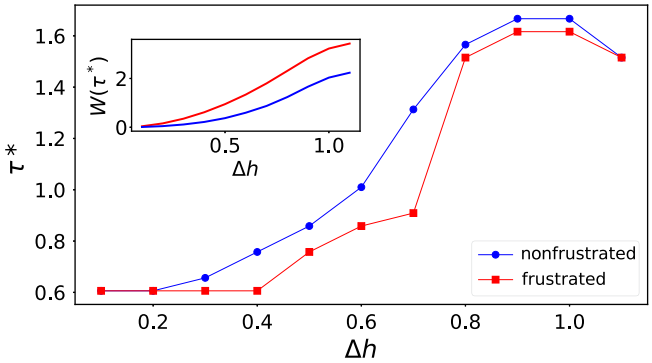


FIG. 8. The position of the first local time maximum $\tau^*$ and the corresponding value of $W$ for the frustrated (red) and nonfrustrated (blue) Ising chain. Data are obtained for a chain of $N = 15$ spins, for $h_0 = 0.001$ and $h_1 - h_0 \in (0.01, 1.2)$ and $\nu = 1$.

battery shows a higher robustness with respect to its nonfrustrated counterpart. Even in the limiting case of $\nu = 0$ (dashed line), the value of $\eta$ is above 0.9 for a frustrated battery, while it drops below 0.5 for the nonfrustrated one. These drops in $\eta$ are more pronounced for larger values of the quench jump $\Delta h$. Indeed, for smaller quenches, the most populated state is still the ground state. Hence, at least in principle, one could still try to get as close as possible to the initial state when discharging the battery. However, this becomes more difficult when increasing $\Delta h$, as the number of excited states that are macroscopically populated increases and therefore the loss of quantum coherence has a stronger impact on the value of the ergotropy and hence of $\eta$.

The decoherence also affects the charging time, making the charging slower for both the frustrated and the nonfrustrated batteries. Therefore, we also extend the analysis carried out in Sec. III to the case of the slow-charging process. The results in Fig. 8 confirm the fact that the charging processes for both frustrated and nonfrustrated systems are comparable but that the virtuous circle we have seen in the fast-charging regime has disappeared. Indeed, while in the fast-charging regime by increasing the quench amplitude $\Delta h$ we would increase the ergotropy of the battery and observe a reduction of the charging time $\tau$, in the slow-charging regime it is still true that the ergotropy increases with the quench amplitude but, instead, the charging time tends to increase, reducing the performance of the quantum battery.

## V. DISCHARGING THE DEVICE

Up to now, we have mainly focused on the ergotropy of the system and how much it could be affected by the presence of an unavoidable nonunitary dynamic that continues to act even after the end of the charging process. However, such a quantity represents an upper bound of energy that can be extracted from a QB, which is hard to approach when this last is represented by a many-body system. Therefore, in this section, we have chosen to analyze a more realistic situation in which the battery can act as an activator for a second quantum device. We take into account a situation in which a QB, after ending the charging process and waiting a time $T \gg \tau_2$ such that its state can be considered completely incoherent, is made to interact with an ancillary two-level system. The Hamiltonian of the total system will therefore read as

$$H_W = J \sum_{k=1}^{N} \sigma_k^x \sigma_{k+1}^x - h \sum_{k=1}^{N} \sigma_k^z + \lambda H_{\text{int}} + \omega \sigma_S^z, \qquad (13)$$

where $\{\sigma_k^\alpha\}_{k=1}^N$ and $\{\sigma_S^\alpha\}$ ($\alpha = x, y, z$) are, respectively, the spin operators of the $k$th site of the QB and the ancillary spin, while $\omega$ is the characteristic energy of the ancillary spin.

To simulate a realistic condition, we consider that only one of the spins of the battery directly interacts with the ancillary system. Moreover, for the same reason, we do not try to optimize the kind of interaction between the QB and the ancillary system, which can give rise to couplings that are extremely hard to simulate, but we directly take into account a realistic interaction terms such as a hopping term. Accordingly, with these assumptions, $H_{\text{int}}$ reads

$$H_{int} = \sigma_1^+ \sigma_S^- + \sigma_1^- \sigma_S^+, \qquad (14)$$

where $\sigma_1^\pm = \sigma_1^x \pm i\sigma_1^y$ and $\sigma_S^\pm = \sigma_S^x \pm i\sigma_S^y$ and the strength of the interaction is parametrized by $\lambda$. Therefore, the ancillary spin is interacting with a single spin in the battery. The interaction that we have chosen breaks both the translational invariance and the parity symmetry of the battery, increasing the number of states accessible during the discharging process. Moreover, it can be experimentally realizable in Rydberg-atom systems [76]. Before going further, let us emphasize that, ideally, one would want an interaction term that commutes with the rest of the combined battery-system Hamiltonian. However, since our battery is a many-body system in which the eigenstates are delocalized, this would require an interaction term that interacts with the battery as a whole. However, such an interaction, even if theoretically achievable, would be unrealistic from an experimental point of view.

In our simulation, we consider that, at time zero, the battery and the ancillary system are brought into contact by turning on the interaction in the equation. Before this, the two systems have been prepared. As far as the QB is concerned, we have at first charged it with the unitary protocol, stopping at the time of the first peak in $\eta$, for $h_0 = 0.018$ and $h_1 = 1.5$, and then let it relax to the diagonal ensemble. On the contrary, the ancillary system is initialized in its lowest-energy state $\rho_S$, i.e., the spin-down configuration, for $\omega = 2|J| = 2$. This value of $\omega$ is chosen in such a way

as to resonate with the band gaps of the battery spectrum, which, for $h_0$ close to the classical point (i.e., $h_0 = 0$), are proportional to $J$. The strength of the interaction between the spin and the battery has been chosen small enough that the interaction does not carry too much energy into the system but strong enough to allow for energy transfer. We have established numerically that $\lambda = 0.02$ is a good compromise that ensures that no appreciable energy is absorbed or released from the interaction term.

Soon after $t = 0$, the global system, initialized in the product state $\rho_B \otimes \rho_s$, is allowed to evolve under the action of global Hamiltonian $H_W$ and the energy starts to flow from the QB to the ancillary system. As for all systems, when some energy is provided to the ancillary spin, a part of it will be stored as work, while the rest will be dissipated as heat. Hence, a crucial question is whether and how much of this energy can be seen as work performed by the QB on the ancillary spin. One way to respond to this question is to analyze the ratio $\kappa$ between the ergotropy $W_S$ acquired by the ancillary spin (which is initialized in a zero-ergotropy state, i.e., its ground state) and its maximal ergotropy, i.e.,

$$\kappa = \frac{W_S}{2\omega}. \tag{15}$$

In other words, $\kappa$ is the amount of energy that can be used later by the ancillary spin to perform some work.

The results obtained through exact diagonalization for $\kappa$, for both the frustrated and nonfrustrated battery, are shown in Fig. 9, for different values of $\Delta h$ and of the size of the chain. The plot shows that none of the energy transferred from the nonfrustrated battery is translated into ergotropy for the ancillary spin. On the contrary, the frustrated battery manages to charge the ancillary spin up to 42% of its maximal ergotropy. This percentage decreases with increasing size of the battery, due to the very local nature of the interaction between the battery and the ancillary spin. Motivated by these impressive results, we have analyzed what happens when we change some conditions such as the values of $h_0$ or $\omega$. The results of this analysis are presented in the Supplemental Material [74] and they show that in most situations it is possible to find a window of values of $\lambda$ in which the frustrated QB has good performance and manages to transfer ergotropy to the ancillary spin. This is not the case for the nonfrustrated battery, which is never able to charge the ancillary qubit with more than heat. Thus, while a certain fine tuning of the interaction strength $\lambda$ is needed to ensure that the energy transferred is not due to the interaction itself, the results presented in Fig. 9 seem quite generic. At this stage, the origin of this striking difference between the frustrated QB and the nonfrustrated one is not clear. While the energy resilience against decoherence can be correlated to the battery energy spectrum, with a higher density of states at low energy in the frustrated case, the data that we have collected, and

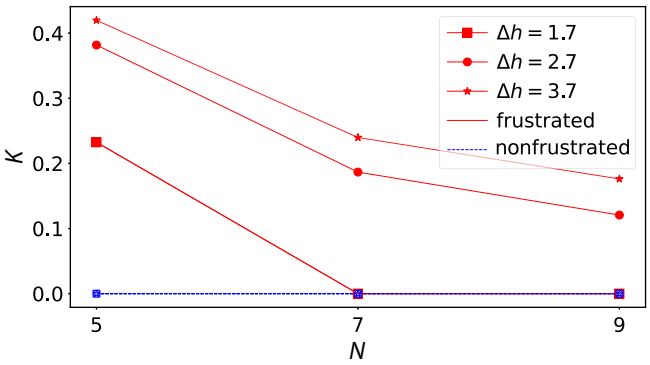


FIG. 9. The ergotropy charged in the ancillary spin from the frustrated battery (full red) and nonfrustrated (empty blue) batteries of $N = 5$, 7, and 9 spins. The results are obtained for $h_0 = 0.02$, $\omega = 2$, $\lambda = 0.02$, and $h_1 = 1.72$, 2.72, and 3.72.

that we partially report in the Supplemental Material [74], indicate that a gapless spectrum is not sufficient to transfer ergotropy during our discharging protocol. We are thus led to speculate that the better performance of the frustrated battery in this respect is due to the peculiar quantum correlations that are characteristic of topological frustration [64,65].

## VI. DISCUSSION AND CONCLUSIONS

Quantum batteries are a critical and rapidly advancing technology, holding the promise of revolutionizing energy storage. While they show great potential and significant progress has been made in terms of scalability, it is essential to acknowledge that quantum batteries are still in their early stages of research and development. In this context, our goal has been to establish the foundation for an alternative approach to QBs that can be used to realize quantum devices that can work as energy activators in quantum technologies, by transferring energy to the quantum devices with which they are interacting. In particular, we have proposed a quantum battery based on a quantum many-body system—namely, the quantum Ising chain—designing a cyclic charging protocol based on a global quench in the external magnetic field to store energy in the battery. We have used different figures of merit to characterize the efficiency of such devices. In every case, we have observed that the frustrated batteries present a very strong resistance to decoherence effects. This remarkable result is related to the fact that the ground state of the frustrated system belongs to a gapless band, allowing for a more efficient energy extraction with respect to the nonfrustrated models, where the presence of a finite gap between the ground state and the rest of the spectrum increases the energy of the final equilibrium state of the battery, therefore reducing the fraction of energy that it is possible to extract. Thus, our results show that topologically frustrated systems can represent a much more

efficient option for the realization of a quantum battery with respect to their nonfrustrated counterparts.

For the ergotropy, we have tested the stability of these results by varying the parameters governing the model ($N$, $h_0$) and the charging protocol ($\Delta h$). In all the measured ranges, we have always observed a higher robustness to decoherence for the frustrated model. In the range of parameters that we have considered, the charging times of the frustrated and nonfrustrated batteries are comparable, even though for some values of the parameter we have observed shorter charging times for the nonfrustrated case. However, even when the nonfrustrated battery is charged a little faster, the frustrated battery still possesses a higher ergotropy and a larger value of $\eta$. We expect these results to be valid even after increasing the system size. Moving toward the thermodynamic limit, one might expect that the value of $\eta$ might decrease, since the system will start populating states in higher-energy bands (this requires more thorough investigation). However, at the same time, the density of states within a band will increase as the gaps tend to close as $N^{-2}$ and for the frustrated system, the degeneracy will always be larger than for the nonfrustrated one. Therefore, also in the thermodynamic limit, we expect the frustrated model to be more robust to decoherence than the nonfrustrated one.

Moreover, we have analyzed what happens in a discharging process in which we connect an ancillary spin to the battery. We have defined a protocol that allows energy transfer from the battery to the spin and measured the level of charge acquired by the spin, as a fraction of its maximal ergotropy $\kappa$. The results show that the energy transferred from the nonfrustrated battery is not translated into ergotropy for the ancillary spin, while, within the considered parameters, the frustrated battery charges the spin up to 42% of the maximal ergotropy, which is $2\omega$. Therefore, topological frustration emerges as a very useful resource to enhance energy transfer from a QB. While the results obtained in Secs. III and IV are solely related to the spectral properties induced by topological frustration, the extent to which the structure of the internal correlations in topologically frustrated chains also plays a role in the energy transfer to an additional system is still unclear. We leave this investigation to future work.

As a final remark, we would like to point out that spin models such as the one-dimensional quantum Ising chain can be experimentally realized with Rydberg atoms. In the currently available experimental platforms, typical values of the couplings are $\tilde{J} \approx \hbar \times 672$ MHz, $\tilde{h} \approx \hbar \times 25$ MHz and the system can be stabilized for times of the order of 20–70 μs. The fastest decoherence time scale of the system can be estimated as the time it takes for the oscillating coherences to average out, i.e., $\tau_d \approx \hbar/(\tilde{J}\Delta E)$, where $\Delta E$ is the largest dimensionless energy difference between the energy eigenstates populated after the quantum quench for the Ising chain described by the dimensionless Hamiltonian $H(1, \tilde{h}/\tilde{J})$. Since $\Delta E$ is of order unity, the typical decoherence time will be of the order of a few tenths of nanoseconds. For the parameters mentioned above, we would have $\tau_d \approx 1.4$ ns. Since this time is considerably smaller than the time for which the system can be stabilized, decoherence effects might become relevant for a quantum battery realized on these platforms. Therefore, because of their high robustness to decoherence, topologically frustrated quantum batteries might represent a valid alternative for the realization of these quantum devices. We leave a more detailed study of a realistic design on Rydberg-atom platforms and of different discharging protocols to future work.

## ACKNOWLEDGMENTS

A.G.C. and O.M. acknowledge support from the Molecular Quantum Simulations (MOQS) Innovative Training Network (ITN) program, a European Union Horizon 2020 research and innovation program under the Marie Skłodowska-Curie Grant Agreement No. 955479. S.M.G. and F.F. acknowledge support from the QuantiXLie Center of Excellence, a project cofinanced by the Croatian Government and the European Union through the European Regional Development Fund—Competitiveness and Cohesion (Grant KK.01.1.1.01.0004). F.F. and S.M.G. also acknowledge support from the Croatian Science Foundation (HrZZ) Project No. IP-2019-4-3321. O.M. acknowledges support from the Julian Schwinger Foundation. V.G. and O.M. acknowledge financial support by the Ministero dell' Università e della Ricerca (Ministry of Education and Research, MUR) through the National Recovery and Resilience Plan (PNRR) project under Grant No. PE0000023-NQSTI.

## APPENDIX A: SOLUTION OF THE ISING MODEL—FRUSTRATED VERSUS NONFRUSTRATED CASE

It is well known that the Ising model in Eq. (1) can be diagonalized exactly. For the sake of simplicity, we limit our analysis to the case with $0 \leq h < 1$ but our results can also be easily extended to the other regions of parameter space. We will consider the case of an odd number of spins $N$ and periodic boundary conditions, i.e., we apply FBCs. In such a way, we can easily switch from the frustrated to the nonfrustrated model by setting $J = 1$ or $J = -1$, respectively. In particular, in the first case, in the presence of an antiferromagnetic interaction between nearest-neighbor spins, frustration has been proven to produce nontrivial modifications to the ground-state properties of the model. The standard procedure prescribes a mapping of spin operators into fermionic ones [63], which are defined

by the Jordan-Wigner transformation:

$$\sigma_j^- = \prod_{l<j} \sigma_l^z \psi_l^\dagger, \quad \sigma_j^+ = \prod_{l<j} \sigma_l^z \psi_j, \quad \sigma_j^z = 1 - 2\psi_j^\dagger \psi_j, \tag{A1}$$

where the $\psi_l$ ($\psi_l^\dagger$) are fermionic annihilation (creation) operators. In terms of such operators, taking into account the periodic boundary conditions and discarding constant terms, the Hamiltonian thus becomes

$$\begin{aligned} H = J \sum_{j=1}^{N-1} \Big[ \psi_{j+1}^\dagger \psi_j + \psi_j^\dagger \psi_{j+1} + \psi_j^\dagger \psi_{j+1}^\dagger + \psi_{j+1} \psi_j \Big] \\ + 2h \sum_{j=1}^{N} \psi_j^\dagger \psi_j - J \Pi^z \Big[ \psi_1^\dagger \psi_N + \psi_N^\dagger \psi_1 + \psi_N^\dagger \psi_1^\dagger \\ + \psi_1 \psi_N \Big], \end{aligned} \tag{A2}$$

where $\Pi^z = \prod_{j=1}^N \sigma_j^z = \prod_{j=1}^N (1 - 2\psi_j^\dagger \psi_j)$ is the parity operator along $z$. The latter expression is not quadratic itself but reduces to a quadratic form in each of the parity sectors of $\Pi^z$. Therefore, it is convenient to write it in the form

$$H = \frac{1+\Pi^z}{2} H^+ \frac{1+\Pi^z}{2} + \frac{1-\Pi^z}{2} H^- \frac{1-\Pi^z}{2},$$

where both $H^\pm$ are quadratic. Hence we can bring the Hamiltonian into a free-fermion form by means of two final steps. First, we perform a Fourier transform

$$\psi_q = \frac{e^{-\imath \pi/4}}{\sqrt{N}} \sum_{j=1}^{N} e^{-\imath q j} \psi_j. \tag{A3}$$

It is worth noting that due to the different quantization conditions, the $H^\pm$ are defined on two different sets of fermionic modes, $q \in \Gamma^- = \{(2\pi n/N)\}_{n=0}^{N-1}$ in the odd sector and $q \in \Gamma^+ = \{(2\pi/N)(n+\frac{1}{2})\}_{n=0}^{N-1}$ in the even one, respectively. Finally a Bogoliubov rotation in Fourier space,

$$b_q = \cos\theta_q \psi_q + \sin\theta_q \psi_{-q}^\dagger, \tag{A4}$$

with momentum-dependent Bogoliubov angles

$$\theta_q = \frac{1}{2} \arctan\left( \frac{\sin q}{h + J\cos q} \right) \; q \neq 0, \pi, \; \theta_{0,\pi} = 0, \tag{A5}$$

leads to the Hamiltonians

$$H^- = \sum_{q \in \Gamma^- / \{0\}} \Lambda(q) \left( b_q^\dagger b_q - \frac{1}{2} \right) + \epsilon(0) \left( b_0^\dagger b_0 - \frac{1}{2} \right), \tag{A6a}$$

$$H^+ = \sum_{q \in \Gamma^+ / \{\pi\}} \Lambda(q) \left( b_q^\dagger b_q - \frac{1}{2} \right) + \epsilon(\pi) \left( b_\pi^\dagger b_\pi - \frac{1}{2} \right). \tag{A6b}$$

Here, $b_q$ ($b_q^\dagger$) are the Bogoliubov annihilation (creation) fermionic operators. The dispersion relation $\Lambda(q)$ for $q \neq 0, \pi$ obeys

$$\Lambda(q) = \sqrt{(h + J\cos q)^2 + J^2 \sin^2 q}, \tag{A7}$$

while for the two specific modes $q = 0 \in \Gamma^-$ and $q = \pi \in \Gamma^+$, we have

$$\epsilon(0) = h + J, \quad \epsilon(\pi) = h - J. \tag{A8}$$

It is important to observe that all the fermionic modes are associated with a positive energy except for the 0 and $\pi$ modes, which carry negative energy for $J = -1$ and $J = 1$, respectively, since we have chosen $h < 1$. Let us start by considering the FM case $J = -1$. In this case, for $0 \leq h < 1$, the only mode that carries negative energy is the 0 mode in the odd sector, while all the modes in the even-parity sector carry positive energy. Therefore, in this case, the ground state is given by a state with a 0-mode populated $b_0^\dagger |\emptyset^-\rangle$ in the odd-parity sector. One can observe that the vacuum states in each sector can be written in terms of the fermionic states $|0,1\rangle_q$ and of the Bogoliubov angles $\theta_q$, and read

$$|\emptyset^+\rangle = |0_\pi\rangle \bigotimes_{q \in \Gamma_2^+} \left( \cos\theta_q |0\rangle_q |0\rangle_{-q} - \sin\theta_q |1\rangle_q |1\rangle_{-q} \right), \tag{A9a}$$

$$|\emptyset^-\rangle = |0_0\rangle \bigotimes_{q \in \Gamma_2^-} \left( \cos\theta_q |0\rangle_q |0\rangle_{-q} - \sin\theta_q |1\rangle_q |1\rangle_{-q} \right), \tag{A9b}$$

where $\Gamma_2^+$ ($\Gamma_2^-$) is the subset of momenta $q \in \Gamma^+$ ( $q \in \Gamma^-$) that lives in the interval $q \in (0, \pi)$. One can explicitly check that the ground-state energy is given by

$$E_0^- = -\frac{1}{2} \sum_{q \in \Gamma^-} \Lambda(q). \tag{A10}$$

Let us now focus on the analysis of the AFM model obtained for $J = 1$. In this case, we observe that the $\pi$ mode is the only one that can be characterized by a negative excitation energy. However, the $\pi$ mode only exists in the even-parity sector, where the addition of a single excitation is forbidden by the parity constraint.

For this reason, the lowest-energy state of the even sector in this region is still its Bogoliubov vacuum $|\emptyset^+\rangle$. In the odd sector, states with a single excitation are allowed but all fermionic modes hold positive energy and it is easy to check that each state that can be defined in this sector has an energy greater than the one associated with $|\emptyset^+\rangle$. Despite this, the lowest admissible states in this sector, those with one occupied mode with momentum closest to $\pi$ (exactly $\pi$ is not possible because of the quantization rule of this sector), have an energy gap closing as $1/N^2$ compared to $|\emptyset^+\rangle$. The ground-state energy is given by

$$E_0^+ = \Lambda(\pi) - \frac{1}{2}\sum_{q\in\Gamma^+}\Lambda(q). \tag{A11}$$

Finally, let us discuss the behavior of the energy gap more quantitatively. The two lowest eigenvalues of the Hamiltonian in Eq. (1), for $J > 0$ and odd $N$, are given by

$$\epsilon_0 = \Lambda(\pi) - \frac{1}{2}\sum_{q\in\Gamma^+}\Lambda(q) \tag{A12}$$

and

$$\epsilon_1 = \Lambda\left(\pi - \frac{\pi}{N}\right) - \frac{1}{2}\sum_{q\in\Gamma^-}\Lambda(q). \tag{A13}$$

For any value of $N$ and $h$, the exact expression of the energy gap is thus given by

$$\begin{aligned}\Delta_{\mathrm{AFM}} &= \epsilon_1 - \epsilon_0 \\ &= \Lambda(\pi) - \Lambda\left(\pi - \frac{\pi}{N}\right) + \frac{1}{2}\left[\sum_{q\in\Gamma^+}\Lambda(q) - \sum_{q\in\Gamma^-}\Lambda(q)\right].\end{aligned} \tag{A14}$$

Sufficiently far from the quantum critical point at $h = 1$, the second term in this expression is known to vanish exponentially with the system size. Therefore, for sufficiently large $N$, the energy gap will scale as

$$\begin{aligned}\Delta_{\mathrm{AFM}} &\approx \frac{\pi^2}{2N^2}\Lambda''(\pi) + o(N^{-4}) \\ &= \frac{|h|}{2(1-|h|)}\frac{\pi^2}{N^2} + O(N^{-4}),\end{aligned} \tag{A15}$$

which coincides with Eq. (2) when setting $J = 1$. Therefore, in the bulk of the AFM phase, the energy gap closes quadratically with the system size.

As we get closer to the critical point, it is no longer true that the second term of Eq. (A14) vanishes exponentially in the system size. Therefore, the expansion that we performed earlier is no longer valid and one expects the gap to close in the same way as it closes in the nonfrustrated critical system, i.e., as $1/N$. However, we would like to highlight the fact that the scaling suggested by Eq. (A15) holds not just for $|h| \ll 1$ but, for large $N$, in the whole bulk of the frustrated region.

## APPENDIX B: PROJECTION COEFFICIENTS AFTER A GLOBAL QUENCH

In this appendix, we compute the projection coefficients analytically after a global quench from a Hamiltonian $H_0 \equiv H(J, h_0)$ to $H_1 \equiv H(J, h_1)$. Since the fermionic structure of the states is the same, the results hold both for the nonfrustrated (FM) and the frustrated (AFM) case. The initial state before the quench is considered to be the ground state of $H_0$. In the FM ($J = 1$) case, this can be given by

$$|G_0^+\rangle = |\emptyset^+\rangle_0 \tag{B1}$$

or

$$|G_0^-\rangle = b_0^\dagger\,|\emptyset^-\rangle_0 = |0\rangle_0\,, \tag{B2}$$

depending on the parity sector, while in the AFM ($J = -1$), the ground state is always in the even sector and we have

$$|G_0^+\rangle = |\emptyset^+\rangle_0\,. \tag{B3}$$

In both situations, since the global quench in the magnetic field preserves the translational invariance and parity of the model, after the quench the initial state will have nonvanishing projection only onto those eigenstates of $H_1$ with its same parity and momentum, i.e., states with zero momentum. Moreover, since all of the eigenstates are constructed by the addition of quasiparticles with a certain quasimomentum $q$ to a fermionic vacuum, it turns out that the projections will be nonzero only onto those states where excitations are added in couples with opposite momentum, i.e., applying the operator $b_q^\dagger b_{-q}^\dagger$ to the ground state. Using simple combinatorics, one could hence easily understand that in a system with $N$ spins, starting from the initial states $|\emptyset^+\rangle$ or $|0\rangle$, the number of states with nonzero projections will be

$$M = \sum_{l=0}^{\frac{N-1}{2}}\binom{\frac{N-1}{2}}{l} = 2^{\frac{N-1}{2}}. \tag{B4}$$

The projections can be computed explicitly by evaluating scalar products between different states. These are easily evaluated when the states are expressed in the fermion basis rather than in the Bogoliubov one, as in Eq. (A9), since the fermionic operators are independent of

the parameters of the Hamiltonian, which will only enter the Bogoliubov angles. Using the notation

$$|\emptyset_k\rangle = \cos\theta_k\,|0\rangle_k\,|0\rangle_{-k} - \sin\theta_k\,|1\rangle_k\,|1\rangle_{-k}\,, \tag{B5}$$

we also have that

$$b_k^\dagger b_{-k}^\dagger\,|\emptyset_k\rangle = \sin\theta_k\,|0\rangle_k\,|0\rangle_{-k} + \cos\theta_k\,|1\rangle_k\,|1\rangle_{-k}\,. \tag{B6}$$

Therefore, because of the selection rules imposed by the global quench, we have only four possibilities for the scalar products after the quench:

$$\langle\emptyset_k^{(1)}|\,|\emptyset_k^{(0)}\rangle = \cos\Delta_k, \tag{B7}$$

$$\langle\emptyset_k^{(1)}|\,b_k^{\dagger(0)}b_{-k}^{\dagger(0)}\,|\emptyset_k^{(0)}\rangle = -\sin\Delta_k, \tag{B8}$$

$$\langle\emptyset_k^{(1)}|\,b_{-k}^{\dagger(1)}b_k^{\dagger(1)}\,|\emptyset_k^{(0)}\rangle = \sin\Delta_k, \tag{B9}$$

$$\langle\emptyset_k^{(1)}|\,b_{-k}^{\dagger(1)}b_k^{\dagger(1)}b_k^{\dagger(0)}b_{-k}^{\dagger(0)}\,|\emptyset_k^{(0)}\rangle = \cos\Delta_k, \tag{B10}$$

where $\Delta_k = \theta_k^{(1)} - \theta_k^{(0)}$.

Finally, we can introduce the notation $|P_0\rangle = \prod_{p\in P_0} b_p^\dagger b_{-p}^\dagger\,|G_0\rangle$, to the describe a generic zero-momentum state, $P_0$ being a subset of $\Gamma^+\setminus\{\pi\}$ or $\Gamma^-\setminus\{0\}$ depending on the parity sector. With this in mind, the projection coefficient that we are looking for will take the form

$$\langle Q_1|\,|P_0\rangle = \prod_{\substack{k_1\in\Gamma\setminus(Q_1\cup P_0\cup\{0,\pi\}),\\ k_2\in Q_1\cap P_0,\\ k_3\in P_0\setminus Q_1,\\ k_4\in Q_1\setminus P_0}} \cos\Delta_{k_1}\cos\Delta_{k_2}(-\sin\Delta_{k_3})\sin\Delta_{k_4}. \tag{B11}$$

for opportune choices of the quasimomenta, these coefficients will correspond to the $\langle\epsilon_k|\,|\mu_\ell\rangle$ appearing in Eq. (12). Therefore, knowing them allows us to compute the populations $P_\ell$.

## APPENDIX C: FORMAL INTEGRATION OF EQ. (5)

In the case in which the system Hamilton $H$ is time independent, the master equation [Eq. (5)] admits analytical integration [72]. To see this, let us write $H$ as

$$H = \sum_\epsilon \Pi_\epsilon \epsilon, \tag{C1}$$

where $\epsilon$ are the eigenvalues of such an operator and $\{\Pi_\epsilon\}_\epsilon$ is the set of orthogonal projectors that decompose the Hilbert space of the system in the associated energy eigenspaces. Exploiting the fact that $\sum_\epsilon \Pi_\epsilon = \mathbb{1}$, $\Pi_\epsilon\Pi_{\epsilon'} = \delta_{\epsilon,\epsilon'}\Pi_\epsilon$, one can then verify that an explicit solution of Eq. (5) is provided by

$$\rho(t) = \Phi_t^{(H)}[\rho(0)] = \sum_{\epsilon,\epsilon'} \Pi_\epsilon\rho(0)\Pi_{\epsilon'} e^{-\frac{(\epsilon-\epsilon')^2}{2\nu}t - i(\epsilon-\epsilon')t}\,, \tag{C2}$$

where $\Phi_t^{(H)}$ is the dynamical superoperator [77]

$$\Phi_t^{(H)}[\cdots] = \sum_{\epsilon,\epsilon'} \Pi_\epsilon\cdots\Pi_{\epsilon'} e^{-\frac{(\epsilon-\epsilon')^2}{2\nu}t - i(\epsilon-\epsilon')t}. \tag{C3}$$

Note that for $t \gg \tau_2$, where $\tau_2$ is the long dephasing time identified in the main text, such evolution induces complete suppression of the off-diagonal terms that involves superpositions associated with energy eigenvectors of different eigenvalues, i.e.,

$$\Phi_t^{(H)}[\cdots]\Big|_{\nu t\gg 1} \quad\longrightarrow\quad \mathcal{D}^{(H)}[\cdots] = \sum_\epsilon \Pi_\epsilon\cdots\Pi_\epsilon. \tag{C4}$$

For the model we are considering, $H$ is equal to $H_1$ for $t\in]0,\tau[$ and to $H_0$ for $t\geq\tau$. Accordingly, we can write

$$\rho(t) = \begin{cases} \Phi_t^{(H_1)}[\rho(0)], & \forall t\in]0,\tau[,\\ \Phi_{t-\tau}^{(H_0)}\left[\Phi_\tau^{(H_1)}[\rho(0)]\right], & \forall t\geq\tau, \end{cases} \tag{C5}$$

which, for $t = T \geq \tau$ such that $T \gg \tau_2$, leads to

$$\rho(T) \simeq \mathcal{D}^{(H_0)}\left[\Phi_\tau^{(H_1)}[\rho(0)]\right], \tag{C6}$$

where $\mathcal{D}^{(H_0)}$ is the dephasing map [see Eq. (C4)] of $H_0$. Equation (11) finally follows from Eq. (C6), observing that under the assumption that the initial state of the QB is the ground state of $H_0$, then all the eigenspaces involved in the writing of both $\Phi_\tau^{(H_1)}$ and $\Phi_{t-\tau}^{(H_0)}$ only involves eigenspaces with zero momentum, which turn out to be nondegenerate (i.e., their associated projectors are all rank 1).


[1] A. Acín, I. Bloch, H. Buhrman, T. Calarco, C. Eichler, J. Eisert, D. Esteve, N. Gisin, S. J. Glaser, F. Jelezko, S. Kuhr, M. Lewenstein, M. F. Riedel, P. O. Schmidt, R. Thew, A. Wallraff, I. Walmsley, and F. K. Wilhelm, The quantum technologies roadmap: A European community view, New J. Phys. **20**, 080201 (2018).

[2] M. F. Riedel, D. Binosi, R. Thew, and T. Calarco, The European quantum technologies flagship programme, Quantum Sci. Technol. **2**, 030501 (2017).

[3] R. Alicki and M. Fannes, Entanglement boost for extractable work from ensembles of quantum batteries, Phys. Rev. E **87**, 042123 (2013).

[4] F. C. Binder, S. Vinjanampathy, K. Modi, and J. Goold, Quantacell: Powerful charging of quantum batteries, New J. Phys. **17**, 075015 (2015).

[5] F. Campaioli, F. A. Pollock, F. C. Binder, L. Céleri, J. Goold, S. Vinjanampathy, and K. Modi, Enhancing the charging power of quantum batteries, Phys. Rev. Lett. **118**, 150601 (2017).

[6] D. Ferraro, M. Campisi, G. M. Andolina, V. Pellegrini, and M. Polini, High-power collective charging of a solid-state quantum battery, Phys. Rev. Lett. **120**, 117702 (2018).

[7] G. M. Andolina, D. Farina, A. Mari, V. Pellegrini, V. Giovannetti, and M. Polini, Charger-mediated energy transfer in exactly solvable models for quantum batteries, Phys. Rev. B **98**, 205423 (2018).

[8] D. Farina, G. M. Andolina, A. Mari, M. Polini, and V. Giovannetti, Charger-mediated energy transfer for quantum batteries: An open-system approach, Phys. Rev. B **99**, 035421 (2019).

[9] G. M. Andolina, M. Keck, A. Mari, M. Campisi, V. Giovannetti, and M. Polini, Extractable work, the role of correlations, and asymptotic freedom in quantum batteries, Phys. Rev. Lett. **122**, 047702 (2019).

[10] K. V. Hovhannisyan, M. Perarnau-Llobet, M. Huber, and A. Acín, Entanglement generation is not necessary for optimal work extraction, Phys. Rev. Lett. **111**, 240401 (2013).

[11] X. Yang, Y.-H. Yang, M. Alimuddin, R. Salvia, S.-M. Fei, L.-M. Zhao, S. Nimmrichter, and M.-X. Luo, Battery capacity of energy-storing quantum systems, Phys. Rev. Lett. **131**, 030402 (2023).

[12] S. Gherardini, F. Campaioli, F. Caruso, and F. C. Binder, Stabilizing open quantum batteries by sequential measurements, Phys. Rev. Res. **2**, 013095 (2020).

[13] D. Rosa, D. Rossini, G. M. Andolina, M. Polini, and M. Carrega, Ultra-stable charging of fast-scrambling SYK quantum batteries, J. High Energy Phys. **2020**, 67 (2020).

[14] S. Tirone, R. Salvia, and V. Giovannetti, Quantum energy lines and the optimal output ergotropy problem, Phys. Rev. Lett. **127**, 210601 (2021).

[15] S. Tirone, R. Salvia, S. Chessa, and V. Giovannetti, Quantum work capacitances, arXiv:2211.02685.

[16] S. Tirone, R. Salvia, S. Chessa, and V. Giovannetti, Work extraction processes from noisy quantum batteries: The role of non local resources, Phys. Rev. Lett. **131**, 060402 (2023).

[17] S. Tirone, R. Salvia, S. Chessa, and V. Giovannetti, Quantum work extraction efficiency for noisy quantum batteries: The role of coherence, arXiv:2305.16803.

[18] R. R. Rodriguez, B. Ahmadi, G. Suarez, P. Mazurek, S. Barzanjeh, and P. Horodecki, Optimal quantum control of charging quantum batteries, New J. Phys. **26**, 043004 (2024).

[19] F. Pirmoradian and K. Mølmer, Aging of a quantum battery, Phys. Rev. A **100**, 043833 (2019).

[20] F. Mazzoncini, V. Cavina, G. M. Andolina, P. A. Erdman, and V. Giovannetti, Optimal control methods for quantum batteries, Phys. Rev. A **107**, 032218 (2023).

[21] P. A. Erdmann, G. M. Andolina, V. Giovannetti, and F. Noé, Reinforcement learning optimization of the charging of a Dicke quantum battery, arXiv:2212.12397.

[22] G. M. Andolina, M. Keck, A. Mari, V. Giovannetti, and M. Polini, Quantum versus classical many-body batteries, Phys. Rev. B **99**, 205437 (2019).

[23] Z. Wang, H. Li, W. Feng, X. Song, C. Song, W. Liu, Q. Guo, X. Zhang, H. Dong, D. Zheng, H. Wang, and D.-W. Wang, Controllable switching between superradiant and subradiant states in a 10-qubit superconducting circuit, Phys. Rev. Lett. **124**, 013601 (2020).

[24] A. Stockklauser, P. Scarlino, J. V. Koski, S. Gasparinetti, C. K. Andersen, C. Reichl, W. Wegscheider, T. Ihn, K. Ensslin, and A. Wallraff, Strong coupling cavity QED with gate-defined double quantum dots enabled by a high impedance resonator, Phys. Rev. X **7**, 011030 (2017).

[25] N. Samkharadze, G. Zheng, N. Kalhor, D. Brousse, A. Sammak, U. C. Mendes, A. Blais, G. Scappucci, and L. M. K. Vandersypen, Strong spin-photon coupling in silicon, Science **359**, 1123 (2018).

[26] S. Haroche, Nobel Lecture: Controlling photons in a box and exploring the quantum to classical boundary, Rev. Mod. Phys. **85**, 1083 (2013).

[27] Y.-Y. Zhang, T.-R. Yang, L. Fu, and X. Wang, Powerful harmonic charging in a quantum battery, Phys. Rev. E **99**, 052106 (2019).

[28] A. Crescente, M. Carrega, M. Sassetti, and D. Ferraro, Charging and energy fluctuations of a driven quantum battery, New J. Phys. **22**, 063057 (2020).

[29] A. Crescente, M. Carrega, M. Sassetti, and D. Ferraro, Ultrafast charging in a two-photon Dicke quantum battery, Phys. Rev. B **102**, 245407 (2020).

[30] A. Crescente, D. Ferraro, M. Carrega, and M. Sassetti, Enhancing coherent energy transfer between quantum devices via a mediator, Phys. Rev. Res. **4**, 033216 (2022).

[31] F.-Q. Dou, Y.-Q. Lu, Y.-J. Wang, and J.-A. Sun, Extended Dicke quantum battery with interatomic interactions and driving field, Phys. Rev. B **105**, 115405 (2022).

[32] F.-Q. Dou, H. Zhou, and J.-A. Sun, Cavity Heisenberg-spin-chain quantum battery, Phys. Rev. A **106**, 032212 (2022).

[33] F. Zhao, F.-Q. Dou, and Q. Zhao, Charging performance of the Su-Schrieffer-Heeger quantum battery, Phys. Rev. Res. **4**, 013172 (2022).

[34] D. Rossini, G. M. Andolina, and M. Polini, Many-body localized quantum batteries, Phys. Rev. B **100**, 115142 (2019).

[35] D. Rossini, G. M. Andolina, D. Rosa, M. Carrega, and M. Polini, Quantum advantage in the charging process of Sachdev-Ye-Kitaev batteries, Phys. Rev. Lett. **125**, 236402 (2020).

[36] J. Q. Quach, K. E. McGhee, L. Ganzer, D. M. Rouse, B. W. Lovett, E. M. Gauger, J. Keeling, G. Cerullo, D. G. Lidzey, and T. Virgili, Superabsorption in an organic microcavity: Toward a quantum battery, Sci. Adv. **8**, eabk3160 (2022).

[37] J. Monsel, M. Fellous-Asiani, B. Huard, and A. Auffèves, The energetic cost of work extraction, Phys. Rev. Lett. **124**, 130601 (2020).

[38] M. Maffei, P. A. Camati, and A. Auffèves, Probing nonclassical light fields with energetic witnesses in waveguide quantum electrodynamics, Phys. Rev. Res. **3**, L032073 (2021).

[39] J. Oppenheim, M. Horodecki, P. Horodecki, and R. Horodecki, Thermodynamical approach to quantifying quantum correlations, Phys. Rev. Lett. **89**, 180402 (2002).
[40] M. Carrega, A. Crescente, D. Ferraro, and M. Sassetti, Dissipative dynamics of an open quantum battery, New J. Phys. **22**, 083085 (2020).
[41] S.-Y. Bai and J.-H. An, Floquet engineering to reactivate a dissipative quantum battery, Phys. Rev. A **102**, 060201(R) (2020).
[42] F. T. Tabesh, F. H. Kamin, and S. Salimi, Environment-mediated charging process of quantum batteries, Phys. Rev. A **102**, 052223 (2020).
[43] S. Ghosh, T. Chanda, S. Mal, and A. Sen(De), Fast charging of a quantum battery assisted by noise, Phys. Rev. A **104**, 032207 (2021).
[44] A. C. Santos, Quantum advantage of two-level batteries in the self-discharging process, Phys. Rev. E **103**, 042118 (2021).
[45] S. Zakavati, F. T. Tabesh, and S. Salimi, Bounds on charging power of open quantum batteries, Phys. Rev. E **104**, 054117 (2021).
[46] G. T. Landi, Battery charging in collision models with Bayesian risk strategies, Entropy **23**, 1627 (2021).
[47] D. Morrone, M. A. C. Rossi, A. Smirne, and M. G. Genoni, Charging a quantum battery in a non-Markovian environment: A collisional model approach, Quantum Sci. Technol. **8**, 035007 (2023).
[48] K. Sen and U. Sen, Noisy quantum batteries, arXiv:2302.07166.
[49] J. Liu, D. Segal, and G. Hanna, Loss-free excitonic quantum battery, J. Phys. Chem. C **123**, 18303 (2019).
[50] A. C. Santos, B. Cakmak, S. Campbell, and N. T. Zinner, Stable adiabatic quantum batteries, Phys. Rev. E **100**, 032107 (2019).
[51] J. Q. Quach and W. J. Munro, Using dark states to charge and stabilize open quantum batteries, Phys. Rev. App. **14**, 024092 (2020).
[52] A. C. Santos, A. Saguia, and M. S. Sarandy, Stable and charge-switchable quantum batteries, Phys. Rev. E **101**, 062114 (2020).
[53] J. Liu and D. Segal, Boosting quantum battery performance by structure engineering, arXiv:2104.06522.
[54] M. B. Arjmandi, H. Mohammadi, and A. C. Santos, Enhancing self-discharging process with disordered quantum batteries, Phys. Rev. E **105**, 054115 (2022).
[55] A. E. Allahverdyan, R. Balian, and T. M. Nieuwenhuize, Maximal work extraction from finite quantum systems, Europhys. Lett. **67**, 565 (2004).
[56] W. Niedenzu, M. Huber, and E. Boukobza, Concepts of work in autonomous quantum heat engines, Quantum **3**, 195 (2019).
[57] M. B. Arjmandi, H. Mohammadi, A. Saguia, M. S. Sarandy, and A. C. Santos, Localization effects in disordered quantum batteries, Phys. Rev. E **108**, 064106 (2023).
[58] T. P. Le, J. Levinsen, K. Modi, M. M. Parish, and F. A. Pollock, Spin-chain model of a many-body quantum battery, Phys. Rev. A **97**, 022106 (2018).
[59] H.-L. Shi, S. Ding, Q.-K. Wan, X.-H. Wang, and W.-L. Yang, Entanglement, coherence, and extractable work in quantum batteries, Phys. Rev. Lett. **129**, 130602 (2022).
[60] R. Shastri, C. Jiang, G.-H. Xu, B. P. Venkatesh, and G. Watanabe, Dephasing enabled fast charging of quantum batteries, arXiv:2402.16999.
[61] M. L. Néel, Propriétées magnétiques des ferrites; Férrimagnétisme et antiferromagnétisme, Ann. Phys. (Paris) **12**, 137 (1948).
[62] in *Lecture Notes in Physics*, edited by U. Schollwöck, J. Richter, D. J. J. Farnell, and R. F. Bishop (Springer, 2008), Vol. 645, https://link.springer.com/book/10.1007/b96825.
[63] F. Franchini, in *Lecture Notes in Physics* (Springer, 2017), Vol. 940, https://link.springer.com/book/10.1007/978-3-319-48487-7.
[64] V. Marić, S. M. Giampaolo, and F. Franchini, Quantum phase transition induced by topological frustration, Commun. Phys. **3**, 220 (2020).
[65] V. Marić, S. M. Giampaolo, and F. Franchini, The frustration of being odd: How boundary conditions can destroy local order, New J. Phys. **22**, 083024 (2020).
[66] A. G. Catalano, D. Brtan, F. Franchini, and S. M. Giampaolo, Simulating continuous symmetry models with discrete ones, Phys. Rev. B **106**, 125145 (2022).
[67] V. Marić, S. M. Giampaolo, and Fabio Franchini, Fate of local order in topologically frustrated spin chains, Phys. Rev. B **105**, 064408 (2022).
[68] S. M. Giampaolo, F. B. Ramos, and F. Franchini, The frustration of being odd: Universal area law violation in local systems, J. Phys. Commun. **3**, 081001 (2019).
[69] V. Marić, G. Torre, F. Franchini, and S. M. Giampaolo, Topological frustration can modify the nature of a quantum phase transition, SciPost Phys. **12**, 075 (2022).
[70] G. Torre, V. Marić, D. Kuić, F. Franchini, and S. M. Giampaolo, Odd thermodynamic limit for the Loschmidt echo, Phys. Rev. B **105**, 184424 (2022).
[71] J. Odavić, T. Haug, G. Torre, A. Hamma, F. Franchini, and S. M. Giampaolo, Complexity of frustration: A new source of non-local non-stabilizerness, SciPost Phys. **15**, 131 (2023).
[72] G. J. Milburn, Intrinsic decoherence in quantum mechanics, Phys. Rev. A **44**, 5401 (1991).
[73] T. Baumgratz, M. Cramer, and M. B. Plenio, Quantifying coherence, Phys. Rev. Lett. **113**, 140401 (2014).
[74] See the Supplemental Material at http://link.aps.org/supplemental/10.1103/PRXQuantum.5.030319 for a discussion on the choice of the charging time and additional analysis of the discharging protocol.
[75] B. Misra and E. C. G. Sudarshan, The Zeno's paradox in quantum theory, J. Math. Phys. **18**, 756 (1977).
[76] D. Barredo, H. Labuhn, S. Ravets, T. Lahaye, A. Browaeys, and C. S. Adams, Coherent excitation transfer in a spin chain of three Rydberg atoms, Phys. Rev. Lett. **114**, 113002 (2015).
[77] F. Petruccione and H.-P. Breuer, *The Theory of Open Quantum Systems* (Oxford University Press, USA, 2007).